Mon. Not. R. Astron. Soc. **371,** 1373–1380 (2006) doi:10.1111/j.1365-2966.2006.10774.x

Cluster number counts dependence on dark energy inhomogeneities and coupling to dark matter

M. Manera[1]⋆ and D. F. Mota[2,3]⋆

[1]*Institut d'Estudis Espacials de Catalunya IEEC/CSIC, F. de Ciencies, TorreC5 par, UAB, Bellaterra, 08193 Barcelona, Spain*
[2]*Institute for Theoretical Astrophysics, University of Oslo, N-0315 Oslo, Norway*
[3]*Department of Physics, University of Oxford, Keble Road, Oxford OX1 3RH*

Accepted 2006 June 28. Received 2006 June 28; in original form 2006 March 13

ABSTRACT

Cluster number counts can be used to test dark energy models. We investigate dark energy candidates which are coupled to dark matter. We analyse the cluster number counts dependence on the amount of dark matter coupled to dark energy. Furthermore, we study how dark energy inhomogeneities affect cluster abundances. It is shown that increasing the coupling reduces significantly the cluster number counts, and that dark energy inhomogeneities increases cluster abundances. Wiggles in cluster number counts are shown to be a specific signature of coupled dark energy models. Future observations could possibly detect such oscillations and discriminate among the different dark energy models.

Key words: galaxies: clusters: general – cosmology: theory – dark matter – large-scale structure of Universe.

1 INTRODUCTION

Observational measurements from supernovae (Perlmutter et al. 1999; Riess et al. 2001, 2004), cosmic microwave background radiation (Spergel et al. 2003) and large-scale structures (Zehavi et al. 2002) strongly indicate the existence of a dark energy component which corresponds to ∼70 per cent of our Universe energy budget and is responsible for its current acceleration. The most popular candidates to dark energy are the vacuum energy, also dubbed the cosmological constant (Carroll, Press & Turner 1992), and scalar fields also known as cosmon or quintessence (Ratra & Peebles 1988a; Wetterich 2001, 2002). The cosmological constant is spatially homogeneous and its equation of state is always a constant. Scalar fields have a time-varying equation of state and are spatially inhomogeneous (Steinhardt, Wang & Zlatev 1999; Steinhardt 2003). Different dark energy candidates have distinctive astrophysical and cosmological imprints. The later are mainly dependent on the time evolution of the equation of state (see e.g. Zlatev, Wang & Steinhardt 1999; Schuecker et al. 2003; Doran, Karwan & Wetterich 2005; Jassal, Bagla & Padmanabhan 2005) and the behaviour of its perturbations (see e.g. Ferreira & Joyce 1998; Wang & Steinhardt 1998; Ma et al. 1999).

The redshift dependence of cluster number counts is a promising tool to discriminate among different dark energy models. Several authors (see e.g. Multamaki, Manera & Gaztanaga 2003; Solevi et al 2006) have already use it to investigate both non-coupled quintessence models: SUGRA (Brax & Martin 1999), RP (Ratra & Peebles 1988b) and non-standard cosmologies: Cardassian models (Freese & Lewis 2002) and DGP models (Dvali, Gabadadze & Porrati 2000). Other groups have also used cluster number counts together with other observables to show how future galaxy cluster surveys would constrain cosmological parameters like the amount of dark energy today or the equation of state parameter (Le Delliou 2006; Wang et al. 2004; Lima & Hu 2004; Haiman Mohr & Holder 2000; Horellou & Berge 2005). The possible effects of dark energy inhomogeneities on cluster abundances was investigated by Nunes, da Silva & Aghanim (2006) for minimally coupled dark energy models. However, so far no one has ever tested dark energy models coupled to dark matter using cluster number counts.

Scalar field candidates to dark energy coupled to dark matter are strongly motivated by extradimensional particle physics models. A general feature of these theories is that the size of the extradimensions is intimately related to a scalar field. The later is coupled to all, or a selection of matter fields (Damour, Gibbons & Gundlach 1990), depending on the high energy physics model (Carroll et al. 1992; Carroll 1998; Bertolami & Mota 1999). A non-minimal coupling of the quintessence field to dark matter is therefore worth investigating (Wetterich 1995; Amendola 2000; Amendola & Tocchini-Valentini 2001; Amendola & Tocchini-Valentini 2002; Tocchini-Valentini & Amendola 2002; Farrar & Peebles 2004; Mainini & Bonometo 2004). It is then natural to think that due to this coupling, inhomogeneities in the dark matter fluid will then propagate to the scalar field, affecting its evolution (Barrow & Mota 2003; Nunes & Mota 2006). Clearly such effect will become even more important when dark matter perturbations become non-linear. Hence, it is interesting to investigate the possibility of a dark energy component which may present inhomogeneities at cluster scales, during the non-linear regime of matter perturbations

⋆E-mail: manera@ieec.uab.es (MM); mota@astro.uio.no (DFM)

(Mota & van de Bruck 2004; Maor & Lahav 2005). In fact, Wetterich (2001, 2002) and in Arbey, Lesgourgues & Salati (2001) speculated that highly non-linear matter perturbations might indeed affect a scalar field even on galactic scales. They found that, at least in principle, the quintessence field (or a scalar field) could be responsible for the observed flat rotation curves in galaxies. In Padmanabhan & Choudhury (2002), Padmanabhan (2002), Bagla, Jassal & Padmanabhan (2003) and Causse (2003) more exotic models, based on tachyon fields, have been discussed and they argued that the quintessence equation of state is scale dependent. This is indeed a general feature of non-minimally coupled scalar fields, whose properties depend on the local density of the region they 'live in' (Khoury & Weltman 2003, 2004a,b; Brax et al. 2004; Clifton, Mota & Barrow 2004; Mota & Barrow 2004a,b).

In this paper we investigate the possibility of using measurements from cluster number counts to differentiate among dark energy models. We study quintessence candidates coupled to dark matter and analyse the cluster number counts dependence on the amount of dark matter coupled to dark energy. Adding to that, we also consider the possibility of dark energy models which present inhomogeneities at cluster scales, during the non-linear regime of structure formation. We then compare with the more popular models where dark energy is homogeneous at those scales and where inhomogeneities only occur at horizon scales. We conclude the article assessing the possibility of near future galaxy surveys to discriminate quintessence models coupled to dark matter.

2 COUPLED QUINTESSENCE AND THE SPHERICAL COLLAPSE

We consider a flat, homogeneous and isotropic background universe with scale factor $a(t)$. Since we are interested in the matter-dominated epoch, when structure formation starts, we assume that the universe is filled with cold dark matter (CDM) and a quintessence field (ϕ). The equation that describes our background universe scale factor is (we set $\hbar = c \equiv 1$ throughout the paper)

$$3H^2 = 8\pi G(\rho_{\rm m} + \rho_\phi), \tag{1}$$

where $H \equiv \dot{a}/a$ is the Hubble rate, $\rho_\phi = (1/2)\dot{\phi}^2 + V(\phi)$ and $V(\phi)$ is the scalar field potential. We assume the potential to be a pure exponential function $V(\phi) = V_0 \exp{(\alpha\kappa\phi)}$, where $\kappa^2 = 8\pi G$. This is widely used in the literature. With the correct choice of the parameter α this potential leads to a late time acceleration (Amendola 2000; Barreiro et al. 2000; Copeland, Nunes & Pospelov 2004; Brookfield et al. 2006). Since we are investigating non-minimally coupled quintessence fields, $\rho_{\rm m}$ includes both the dark matter coupled to dark energy ($\rho_{\rm cDM}$) as well as the non-coupled dark matter ($\rho_{\rm um}$). Throughout all the paper we use $\Omega_{\rm m0} = 0.3$, $\Omega_{\phi 0} = 0.7$ and $h = 0.65$.

It is important to note that our theory differs significantly in one key aspect from the work of Kaplinghat & Rajaraman (2006), where instabilities in the matter fluid can occur. In our models, the dark energy sector is described by a *light* scalar field, with a mass which is at most of order H. The models investigated by Kaplinghat & Rajaraman (2006) are such that the mass of the scalar field is much larger than H for most of its history. This can have significant implications upon the behaviour of the dark matter background and the growth of perturbations which may lead to instabilities.

In order to calculate cluster abundances we need the evolution of the linear matter density contrast (δ). We describe the evolution of an overdensity up to the non-linear regime using the spherical collapse model (see e.g. Padmanabhan 1995). The radius of the overdense region r and density contrast δ are related in this case by $1 + \delta = \rho_{\rm mc}/\rho_{\rm m} = (a/r)^3$, where $\rho_{\rm mc}$ and $\rho_{\rm m}$ are the energy densities of pressureless matter in the cluster and in the background, respectively.

The energy density of cold dark matter in the background and inside the collapsing region are simply given by the following analytical solutions (see e.g. Amendola 2000):

$$\rho_{\rm um} = \rho_0\Omega_{\rm um0}\left(\frac{a_0}{a_i}\right)^3\left(\frac{a_i}{a}\right)^3, \tag{2}$$

$$\rho_{\rm cDM} = \rho_0\Omega_{\rm DM0}\left(\frac{a_0}{a_i}\right)^3\left(\frac{a_i}{a}\right)^3 {\rm e}^{B(\phi)-B(\phi_0)}, \tag{3}$$

$$\rho_{\rm umc} = (1+\delta_i)\rho_0\Omega_{\rm um0}\left(\frac{a_0}{a_i}\right)^3\left(\frac{r_i}{r}\right)^3, \tag{4}$$

$$\rho_{\rm cDMc} = (1+\delta_i)\rho_0\Omega_{\rm cDM0}\left(\frac{a_0}{a_i}\right)^3\left(\frac{r_i}{r}\right)^3 {\rm e}^{B(\phi_{\rm c})-B(\phi_0)}, \tag{5}$$

where again the subscripts 'um' and 'cDM' mean uncoupled matter and *coupled* dark matter, respectively. Uncoupled matter corresponds to both baryons and uncoupled dark matter. The function $B(\phi)$ represents the coupling between dark energy and dark matter. We use the same coupling as in the model discussed in (Holden & Wands 2000; Amendola 2000), $B(\phi) = -C\kappa\phi$, where C is a constant. Since our scalar field only couples to dark matter, this constant sets the ratio of the strength of the dark–dark interaction with respect to the gravitational interaction; it is then clearly not constrained by local experiments or by $\dot{G}/G$ measurements.[1] However, it is constrained by primordial nucleosynthesis bounds on the quintessence energy density at that epoch. Notice that if the baryons were coupled to the scalar field as well, then we would need to consider several constraints on the coupling which would arise from a variety of experiments and observations of fifth force effects (Ellis et al. 1989; Wetterich 1995).

The total energy densities in the background and inside the cluster are, respectively, $\rho_{\rm m} = \rho_{\rm um} + \rho_{\rm cDM}$ and $\rho_{\rm mc} = \rho_{\rm umc} + \rho_{\rm cDMc}$ which evolve accordingly to

$$\dot{\rho}_{\rm m} = -3\frac{\dot{a}}{a}\rho_{\rm m} + \frac{{\rm d}B}{{\rm d}\phi}\rho_{\rm cDM}\dot{\phi}, \tag{6}$$

$$\dot{\rho}_{\rm mc} = -3\frac{\dot{r}}{r}\rho_{\rm mc} + \frac{{\rm d}B}{{\rm d}\phi_{\rm c}}\rho_{\rm cDMc}\dot{\phi}_{\rm c}. \tag{7}$$

The equations of motion for the evolution of the scalar field in the background and inside the overdensity are in this case (Nunes & Mota 2006):

$$\ddot{\phi} = -3\frac{\dot{a}}{a}\dot{\phi} - \frac{{\rm d}V}{{\rm d}\phi} - \frac{{\rm d}B}{{\rm d}\phi}\rho_{\rm cDM}, \tag{8}$$

$$\ddot{\phi}_{\rm c} = -3\frac{\dot{r}}{r}\dot{\phi}_{\rm c} - \frac{{\rm d}V}{{\rm d}\phi_{\rm c}} - \frac{{\rm d}B}{{\rm d}\phi_{\rm c}}\rho_{\rm cDMc} + \frac{\Gamma_\phi}{\dot{\phi}_{\rm c}}, \tag{9}$$

where Γ_ϕ describes the quintessence loss of energy inside the cluster (see e.g. Mota & van de Bruck 2004; Maor & Lahav 2005).

[1] Damour et al. (1990) derived a constraint for dark matter interaction with a dilaton based on the age of the Universe. This constraint assumes a field with *no* potential and a nowadays matter-dominated universe, which is clearly not our case.

It is known that the system quintessence coupled to dark matter has a scaling attractor solution (Amendola 2000; Holden & Wands 2000; Amendola & Tocchini-Valentini 2002a) with

$$\Omega_\phi = \frac{C^2 + C\alpha + 3\gamma}{(C+\alpha)^2}, \qquad \gamma_\phi = \frac{3\gamma^2}{C^2 + C\alpha + 3\gamma}, \tag{10}$$

where γ and γ_ϕ are the background and the scalar field equation of state, respectively. This attractor has a power-law expansion $a \propto t^p$ given by $p = (2/3\ \gamma)\ (1 + (C/\alpha))$ (Copeland et al. 2004). The solution leads to a late time acceleration for $p > 1$, that is for $\alpha < 2C$ for a matter background. The value of C can be extracted from equation (10) where now we also have to take into account the coupled and the uncoupled dark matter. Therefore,

$$C = -\alpha + \frac{\alpha + \sqrt{\alpha^2 - 12\tilde{\Omega}_{\rm cDM}}}{2\tilde{\Omega}_{\rm cDM}} \tag{11}$$

is a good estimate for the value of the coupling in the tracker regime. Here $\tilde{\Omega}_{\rm cDM} = \Omega_{\rm cDM}/(\Omega_{\rm cDM} + \Omega_\phi)$.

The constraints from nucleosynthesis imply that $\Omega_\phi(\tau_{\rm ns}) < 0.1$ (Wetterich 1995; Sarkar 1996; Ferreira & Joyce 1998), which translates into $\alpha^2 > 4/\Omega_\phi(\tau_{\rm ns})$ (Holden & Wands 2000). In all our models we choose $\alpha = 10$, and C will be chosen according to equation (11).

Following Maor & Lahav (2005) and Mota & van de Bruck (2004), we study the two extreme limits for the evolution of dark energy inside the overdensity. In the first case we assume that dark energy is homogeneous, i.e. the value of ρ_ϕ inside the cluster is the same as in the background, with

$$\Gamma_\phi = -3\left(\frac{\dot{a}}{a} - \frac{\dot{r}}{r}\right)(\rho_{\phi_{\rm c}} + p_{\phi_{\rm c}}). \tag{12}$$

Hence, in this case, dark energy perturbations are not present at small scales and so $\phi_{\rm c} = \phi$. In the second limit, dark energy is inhomogeneous and collapses with dark matter. Thus $\Gamma_\phi = 0$ and $\phi_{\rm c} \neq \phi$. In this case perturbations in the scalar field are important at cluster scales.

In order to compute the cluster number counts we also need the evolution for the linear density contrast ($\delta_{\rm L}$) which is given by

$$\ddot{\delta}_{\rm L} = -2H(\dot{\delta}_{\rm L} - f) + \dot{f} + \frac{\kappa^2}{2}\left[\rho_{\rm m}\delta_{\rm L} + \left(1 + 3w_{\phi_{\rm c}}\right)\delta_\phi\ \rho_\phi + 3\rho_\phi\delta w_\phi\right], \tag{13}$$

where $\delta_\phi = \delta\ \rho_\phi/\rho_\phi$, with

$$\delta\rho_\phi = \dot{\phi}\ \delta\dot{\phi} + \frac{{\rm d}V}{{\rm d}\phi}\ \delta\phi, \tag{14}$$

$$\delta w_\phi = (1 - w_\phi)\left(-\frac{1}{V}\frac{{\rm d}V}{{\rm d}\phi}\ \delta\phi + \delta_\phi\right) \tag{15}$$

and

$$f = G\left[\frac{{\rm d}B}{{\rm d}\phi}\ \delta\dot{\phi} + \left(\frac{{\rm d}B}{{\rm d}\phi}\right)^2(1-G)\dot{\phi}\ \delta\phi + \frac{{\rm d}^2B}{{\rm d}\phi^2}\ \dot{\phi}\ \delta\phi\right], \tag{16}$$

where

$$G(\phi) = \frac{\Omega_{\rm cDM0}{\rm e}^{B(\phi)-B(\phi_0)}}{\Omega_{\rm cDM0}{\rm e}^{B(\phi)-B(\phi_0)} + \Omega_{\rm um0}}. \tag{17}$$

This system of equations closes with the equation of motion for the scalar field perturbations:

$$\delta\ddot{\phi} = -3H\ \delta\dot{\phi} - \frac{{\rm d}B}{{\rm d}\phi}\ G\ \rho_{\rm m}\delta_{\rm L} + (\dot{\delta}_{\rm L} - f)\dot{\phi} - \left[\frac{{\rm d}^2V}{{\rm d}\phi^2} + \left(\frac{{\rm d}B}{{\rm d}\phi}\right)^2 G\,(1-G)\,\rho_{\rm m} + \frac{{\rm d}^2B}{{\rm d}\phi^2}\ G\ \rho_{\rm m}\right]\delta\phi. \tag{18}$$

Integrating these equations we are now able to obtain the growth factor $D(z) = \delta_{\rm L}(z)/\delta(0)$ and the linearly extrapolated density threshold above which structures will end up collapsing, i.e. $\delta_{\rm c}(z) = \delta_{\rm L}(z = z_{\rm col})$. Here $z_{\rm col}$ is the redshift at which the radius, r, of the overdensity is zero, and is obtained using the spherical infall model. Both of these quantities are needed to compute the number of collapsed structures following the Press–Schechter formalism (Press & Schechter 1974).

In order to understand the cluster number counts dependence on the amount of dark matter coupled to dark energy and the behaviour of dark energy inhomogeneities during the non-linear regime, we investigate four different models/cases. We have chosen the models parameters in such a way as to have limiting cases. These give us a good understanding of the physics behind large-scale structure formation and coupled quintessence models, being at the same time viable cosmological models. We clarify here the four cases under study.

(i) Model A (homogeneous dark energy with a large amount of dark matter coupled):
All the dark matter is coupled to dark energy, $\Omega_{\rm cDM} = 0.25$. Only baryons remain uncoupled $\Omega_{\rm um} = \Omega_{\rm b} = 0.05$. From equation (11) one has $C = 27.4$. In this model we consider that dark energy does not cluster in overdense regions. Its energy density is the same both in the cluster and in the background. Thus Γ_ϕ is the same as in equation (12).

(ii) Model B (homogeneous dark energy with a small amount of dark matter coupled):
Only a small fraction of the dark matter is coupled, $\Omega_{\rm cDM} = 0.05$. The rest is uncoupled matter $\Omega_{\rm um} + \Omega_{\rm b} = 0.25$. From equation (11) one has $C = 139.9$. As in case A, we consider that dark energy does not cluster in overdense regions. Hence, it is a homogeneous component, with the same density all over the Universe.

(iii) Model C (inhomogeneous dark energy with a large amount of dark matter coupled):
All the dark matter is coupled to dark energy $\Omega_{\rm cDM} = 0.25$, only baryons remain uncoupled $\Omega_{\rm um} = \Omega_{\rm b} = 0.05$. From equation (11), one has $C = 27.4$. In this case we consider that dark energy clusters in overdense regions. Hence, $\Gamma_\phi = 0$, which means that dark energy collapses along with dark matter.

(iv) Model D (inhomogeneous dark energy with a small amount of dark matter coupled):
Only a small fraction of the dark matter is coupled $\Omega_{\rm cDM} = 0.05$. The rest is uncoupled matter $\Omega_{\rm um} + \Omega_{\rm b} = 0.25$. From equation (11) one has $C = 139.9$. As in case C, we also consider the clustering of dark energy in overdense regions, therefore, $\Gamma_\phi = 0$.

In Fig. 1 we have plotted $\delta_{\rm c}(z)$ for several dark matter/dark energy couplings and for both homogeneous and inhomogeneous dark energy models. It is interesting to note the wiggles in $\delta_{\rm c}$, which are a feature of dark energy models coupled to dark matter. These wiggles come from the oscillations in the dark energy scalar field around the minimum of the effective potential. When allowing dark energy to clump with dark matter $\Gamma_\phi = 0$ (inhomogeneous models), these oscillations are strongly translated to the matter fluctuations and hence appear in $\delta_{\rm c}$. Notice that in the homogeneous scenario oscillations are still present (see fig. 5 in Nunes & Mota 2006); nevertheless they are very suppressed and could not be appreciated in the plot.

3 PRESS–SCHECHTER FORMALISM

Press and Schechter (Press & Schechter 1974), using the spherical collapse model, provided a formalism to predict the number density

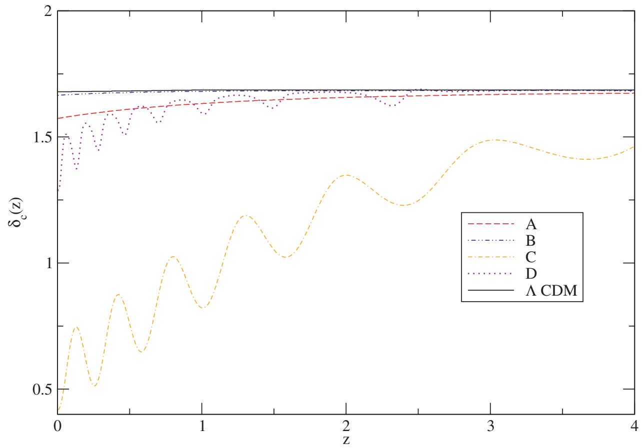

Figure 1. Evolution of δ_c with redshift. Model A: $\Gamma_\phi \neq 0, \Omega_{\rm cDM} = 0.25, \Omega_{\rm um} = \Omega_{\rm b} = 0.05$. Model B: $\Gamma_\phi \neq 0, \Omega_{\rm cDM} = 0.05, \Omega_{\rm um} + \Omega_{\rm b} = 0.25$. Model C: $\Gamma_\phi = 0, \Omega_{\rm cDM} = 0.25, \Omega_{\rm um} = \Omega_{\rm b} = 0.05$. Model D: $\Gamma_\phi = 0, \Omega_{\rm cDM} = 0.05, \Omega_{\rm um} + \Omega_{\rm b} = 0.25$. The ΛCDM case, solid line, is also plotted for reference.

of collapsed objects. Several groups (Gross et al. 1998; Governato et al. 1999; Jenkins et al. 2001; Springel et al. 2005) found significant deviations between Press–Shcecther predictions and *N*-body simulations. A better agreement to the simulations is given, for instance, by the Sheth & Tormen (1999) or Jenkins et al. (2001) fits for $n(m)$. However, the formalism by Press & Schechter (1974) and its extensions by Bond et al. (1991) and Lacey & Cole (1993), even if crude, predicts the evolution of the mass function of collapsed objects well enough for the purpose of this paper: the study of how dark energy inhomogeneities and dark matter–dark energy coupling influences cluster number counts.

The main assumption in the Press and Schechter formalism is Gaussianity of the matter density field. When the density fluctuation field $\delta(\boldsymbol{x})$ is smoothed with a top hat window of radius R, i.e. when averaged in a sufficiently large volume $V = (4\pi/3)R^3$ around each point, it follows a Gaussian distribution:

$$p(\delta_{\rm L}, R) = \frac{1}{\sqrt{2\pi}\sigma} {\rm e}^{-\frac{\delta_{\rm L}^2}{2\sigma^2}}, \tag{19}$$

where $\sigma(R)$ is the rms of linear fluctuations $\delta_{\rm L}$. Both $\sigma(R)$ and $\delta_{\rm L}$ are redshift dependent. The volume fraction of points with $\delta_{\rm L} \geqslant \delta_{\rm c}$ is

$$f = \int_{\delta_{\rm c}}^{\infty} p(\delta_{\rm L}, R){\rm d}\delta_{\rm L} = \frac{1}{2}{\rm erfc}\left(\frac{\delta_{\rm c}}{\sqrt{2}\,\sigma(R)}\right), \tag{20}$$

which is assumed to be equal to the mass fraction in bounded objects with $M \geqslant (4\pi/3)\rho_{\rm m} R^3$.

We are interested in the comoving number density of collapsed objects in a mass range. To obtain this we have to take the derivative of f, which gives the mass fraction in objects with mass between M and $M + {\rm d}M$, and also multiply by $\bar{\rho}/M$, which converts the result into number densities. Here $\bar{\rho}$ is the comoving matter density. Thus, the prediction of the Press–Schechter formalism for the comoving number density of collapsed objects is

$$\begin{aligned} n(M){\rm d}M &= 2\frac{\bar{\rho}}{M}\frac{{\rm d}f}{{\rm d}\sigma}\frac{{\rm d}\sigma}{{\rm d}M}{\rm d}M \\ &= -\sqrt{\frac{2}{\pi}}\left(\frac{\delta_{\rm c}}{\sigma}\right)\frac{{\rm d}\ln\sigma}{{\rm d}\ln M}\exp\left(-\frac{\delta_{\rm c}^2}{2\sigma^2}\right)\frac{\bar{\rho}\,{\rm d}M}{M^2}. \end{aligned} \tag{21}$$

Note that there is a factor of 2 introduced to recover the mean matter density. This factor can be better understood when taking into account the 'cloud-in-cloud' structure of haloes (Bond et al. 1991).

There seems to be some confusion in the literature regarding equation (21). We would like to stress that the matter density $\bar{\rho}(z)$ in this equation is the *comoving* mean matter density at a given redshift. In most cases, it is constant and is equal to the *present* mean matter density, but not always. This equivalence is no longer true when one generalizes the Press–Schechter formalism to coupled quintessence models. In this case one has to bear in mind that $\bar{\rho}$ varies with redshift directly affecting the prediction of the number density of collapsed objects.

Following Viana & Liddle (1999) we take the variance in spheres of radius R to be

$$\sigma(R, z) = \sigma_8 \left(\frac{R}{8\,h^{-1}\,{\rm Mpc}}\right)^{-\gamma(R)} D(z), \tag{22}$$

where $D(z)$ is the growth factor and

$$\gamma(R) = (0.3\Gamma + 0.2)\left[2.92 + \log_{10}\left(\frac{R}{8\,h^{-1}\,{\rm Mpc}}\right)\right], \tag{23}$$

where Γ is the shape parameter of the transfer function. Note that although the formalism by Viana & Liddle (1999) could be crude for the present day precision cosmology experiments, it is good enough for the Press–Schechter formalism and for the purposes of this paper. We are not seeking exact solutions nor precise confrontations with the observational data, but to understand the influence of inhomogeneities in dark energy and dark energy–dark matter interaction on cluster number counts.

As in Sugiyama (1995) we use

$$\Gamma = \Omega_{\rm m} h \exp\left(-\frac{\Omega_{\rm b}(1 + \sqrt{2h})}{\Omega_{\rm m}}\right), \tag{24}$$

because it takes into account the baryon component.

The Press–Schechter formalism gives us the comoving number density of haloes, which we want to compare with astronomical data. In order to make this comparison easier we convert $n(m)$ to a cluster number counts per redshift and square degree with mass $M_{\rm min}$ above $2 \times 10^{14}\,{\rm M}_\odot\,h^{-1}$,

$$\frac{{\rm d}N}{{\rm d}z} = \int_{1\,{\rm deg}^2} {\rm d}\Omega \frac{{\rm d}V}{{\rm d}z\,{\rm d}\Omega}\int_{M_{\rm min}}^{\infty} n(M)\,{\rm d}M. \tag{25}$$

The comoving volume element per unit redshift, ${\rm d}V/{\rm d}z = {\rm d}\Omega r(z)^2/H(z)$ (with $r(z)$ being the comoving distance), depends strongly on the cosmological parameters and, as we will see, on the coupling between dark matter and dark energy. Therefore, it plays an important role on determining the total amount of cluster number counts.

In Fig. 2 we plot $\delta_{\rm c}/\sigma_8\,D$ as a function of redshift for several case scenarios. We find that all coupled models have a ratio $\delta_{\rm c}/\sigma_8\,D$ below that of the ΛCDM model. For non-coupled models this is the only relevant quantity and it would have meant to expect larger halo densities than the ΛCDM model. For coupled quintessence models, however, one has also to take into account the redshift evolution of the comoving matter density, which plays a very important role as we will see in the next section. In fact, $\bar{\rho}$ enters both linearly and also through $\sigma(R(M, \bar{\rho}))$ in the equation for the comoving number density of collapsed objects (see equation 21).

It is interesting to notice that both $\delta_{\rm c}$ and D acquire oscillations through equation (13). Hence, the typical prominent wiggles we saw

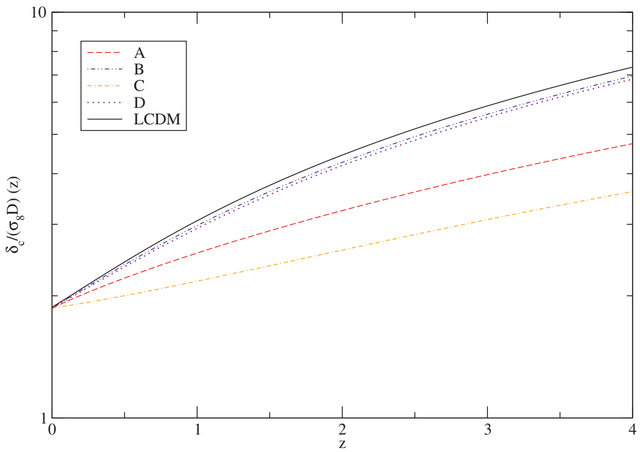

Figure 2. Evolution of the ratio $\delta_c/\sigma_8\, D$ with redshift. Model A: $\Gamma_\phi \neq 0, \Omega_{\mathrm{cDM}} = 0.25, \Omega_{\mathrm{um}} = \Omega_{\mathrm{b}} = 0.05$. Model B: $\Gamma_\phi \neq 0, \Omega_{\mathrm{cDM}} = 0.05, \Omega_{\mathrm{um}} + \Omega_{\mathrm{b}} = 0.25$. Model C: $\Gamma_\phi = 0, \Omega_{\mathrm{cDM}} = 0.25, \Omega_{\mathrm{um}} = \Omega_{\mathrm{b}} = 0.05$. Model D: $\Gamma_\phi = 0, \Omega_{\mathrm{cDM}} = 0.05, \Omega_{\mathrm{um}} + \Omega_{\mathrm{b}} = 0.25$. The ΛCDM case is also plotted for reference.

in δ_c (see Fig. 1) for inhomogeneous coupled dark energy models, cannot be seen in Fig. 2. The reason being that oscillations in δ_c are exactly compensated by oscillations in the linear growth factor when calculating the ratio $\delta_c/\sigma_8\, D$.

4 CLUSTERS NUMBER COUNTS DEPENDENCES

We choose to normalize all models by fixing the number density of haloes $n(m)$ at redshift zero. This is the normalization taken by Nunes et al. (2004). At redshift zero all models have the same comoving background density $\bar{\rho}$ and growth factor D. Therefore, the only dependence on $n(m)$ is through $\delta_c(0)/\sigma_8$ (see equation 21). The normalization is done by adjusting σ_8 in each model such that $\delta_c(0)/\sigma_8$ is equal to the fiducial ($\sigma_8 = 0.9$) ΛCDM case. The table of computed σ_8 is presented below.

Model	σ_8
ΛCDM (fiducial)	0.9
A (homogeneous, large amount coupled)	0.843
B (homogeneous, small amount coupled)	0.892
C (inhomogeneous, large amount coupled)	0.224
D (inhomogeneous, small amount coupled)	0.695

4.1 Dependence on the coupling between dark matter and dark energy

The coupling between dark matter and dark energy results into several signatures which distinguish these models from the minimally coupled ones. The first imprint is associated to the comoving density. In non-coupled dark energy models, as the universe evolves, the mean matter density of the universe (ρ_{m}), gets diluted by a^{-3} due to the expansion. In order to account for the expansion effect one constructs the comoving matter density $\bar{\rho} = \rho_{\mathrm{m}} a^3$. For models with no coupling between dark matter and dark energy, $\bar{\rho}$ remains constant. However, this is not the case for coupled quintessence models, as can be seen from equation (6).

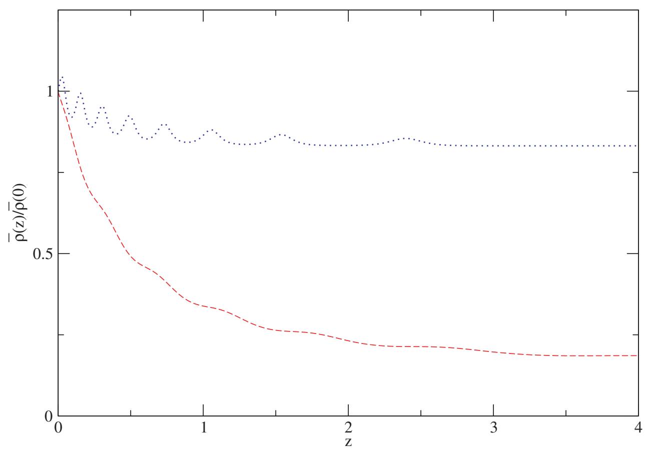

Figure 3. Comoving background matter density as a function of redshift. There is a decrease of density because of the coupling between dark matter and dark energy. Increasing the coupling leads to a faster decreasing of the comoving density with redshift. Wiggles are a characteristic signature of coupled quintessence models. Notice that in this plot non-coupled dark energy models would correspond to a constant line equal to one.

In Fig. 3 we plot the comoving matter density, in units of its present value, as a function of redshift. We can see that $\bar{\rho}$ decreases with redshift. For models with all dark matter coupled to dark energy, $\bar{\rho}$ is reduced a factor of 3 at redshift 1. Since $n(m)$ depends linearly on $\bar{\rho}$, the cluster number counts are reduced by the same factor.

Coupling dark matter to dark energy not only changes $\bar{\rho}$ but also the expansion history of the universe through equation (1) (see e.g. Amendola 2000; Amendola & Tocchini-Valentini (2002a) for the evolution of background quantities). In Fig. 4 we plot the value of $\mathrm{d}V/\mathrm{d}z$ for our models A, B, C and D referenced to the Einstein–de-Sitter universe. The concordance ΛCDM model is also plotted for comparison. Note that the volume element is a background quantity, therefore, the clustering of dark energy during the non-linear regime of matter perturbations does not affect it at all. It is clear from the figure that different possible expansions of the universe are reflected in the comoving volume element evolution with

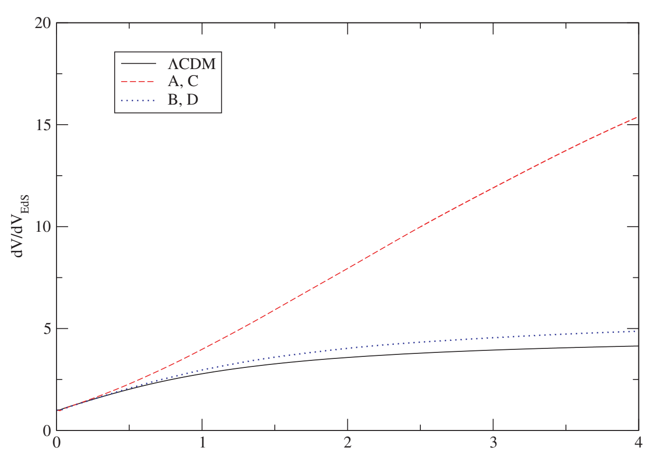

Figure 4. Comoving volume compared to Einstein–de Sitter volume for the four study models. Since the dark energy clustering does not affect the background evolution the difference is due only to the coupling. Models A and C with all dark matter coupled to dark energy have much more volume than models B and D, in which only a small fraction of dark matter is coupled. The concordance ΛCDM model is also plotted for comparison.

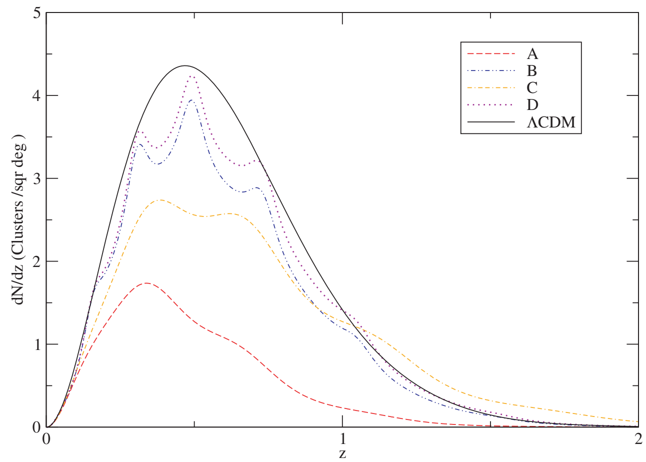

Figure 5. Redshift dependence of the number of clusters of $M > 2 \times 10^{14}\,\mathrm{M}_{\odot}\,h^{-1}$ for square degree. All models are normalized to have the same number density of haloes today. ΛCDM case is also plotted for reference. Note the wiggles which are a feature of coupled dark energy models.

redshift. Models with more dark matter coupled to dark energy have higher values of $\mathrm{d}V/\mathrm{d}z$.

Increasing the value of $\mathrm{d}V/\mathrm{d}z$ directly translates into increased cluster number counts. In fact, this effect is going in the reverse direction to the previous discussed one, i.e. increasing the volume element actually compensates or even overtakes the reduction of the number counts due to a decrease in the comoving density $\bar{\rho}$. The combination of both effects can be more clearly seen in Fig. 5, where the cluster number counts for square degree are plotted for the four models. The ΛCDM model is also plotted for comparison. In this figure, one can see that coupled quintessence models have less number counts than the fiducial ΛCDM. Actually, increasing the amount of dark matter coupled to dark energy leads to a decrease in the number counts obtained. This is due to the different $\delta_{\mathrm{c}}(z)/\sigma(M, z)$ values and the decrease of the comoving matter density, which becomes more important than the larger accessible volume.

A peculiarity of models where dark energy is coupled to dark matter is the oscillations present at the cluster number counts (see Fig. 5). Wiggles are in fact a common characteristic of coupled quintessence models. These appear when the scalar field oscillates about the minimum of its effective potential. Due to the coupling to dark matter, these oscillations are transferred to the dark matter fluid, and induce a corresponding oscillation in the ρ_{cDM} and ρ_{cDMc} components (see fig. 7 of Copeland et al. 2004). Notice, however, that these wiggles are related to the quintessence potential form and initial conditions for the scalar field (Mota & van de Bruck 2004; Nunes & Mota 2006). For instance, other coupled quintessence models which would have an effective potential without a minimum may not present such wiggles. Similarly, a different choice of initial conditions for the scalar field may lead to the case where the field did not have time to reach the minimum of its potential today. Hence, one would not see the oscillations. Nevertheless, fluctuations in the cluster number counts if detected would likely indicate the existence of a coupling between dark energy and dark matter.

4.2 Dependence on the dark energy inhomogeneities

From Fig. 5, it is clear that models with clustering dark energy (inhomogeneous models) have more number counts than their homogeneous counterparts. This can be understood looking at δ_{c} and the ratio $\delta_{\mathrm{c}}(z)/\sigma_8\, D(z)$ (see Figs 1 and 2). When dark energy clusters with matter, it acts as a negative pressure slowing the growth of structures. Models with a linear growth factor increasing slowly have more structure in the past because we normalize all cases such that we have the same number density of haloes today. In fact, the density of collapsed objects is very sensitive to the linear growth factor and to the critical density $\delta_{\mathrm{c}}(z)$. For inhomogeneous dark energy models, it turns out to be significantly lower than the fiducial ΛCDM model (see Fig. 1). This is also the reason for their low σ_8 in the normalization table.

Wiggles are a common feature for both the homogeneous and inhomogeneous cases. There are, however, some differences between these cases. While in homogeneous models wiggles are basically only present in background quantities, i.e. $\bar{\rho}_{\mathrm{m}}$ (see Fig. 3); in the inhomogeneous cases, this is not so. Due to the clustering of dark energy, wiggles will also quite distinctly appear in clustered related quantities like δ_{c} and the linear growth factor δ_{L} (see Fig. 1). Independent of the clustering properties of dark energy, oscillations in cluster number counts will appear, in coupled quintessence models, due to oscillations in the background density. These oscillations are propagated via the Press–Schechter formalism. Since for a given radius of a top hat filter, the volume fraction of the density field points with $\delta_{\mathrm{L}} > \delta_{\mathrm{c}}$ corresponds to the mass fraction of collapsed objects with mass $M > 4/3\pi R^3 \bar{\rho}$. The mass fraction is then converted to number density through the background density.

5 DISCRIMINATING MODELS WITH FUTURE SURVEYS

It is important to estimate whether future surveys measuring cluster abundances will be able to discriminate among different dark energy models. In order to assess such possibility we test our dark energy model B: homogeneous dark energy component with a small amount of dark matter coupled. The aim here is not to perform a detailed analysis but to get an idea of the potential detectability of the features of coupled quintessence models.

Bahcall & Bode (2003) have used the abundance of massive clusters ($m > 8 \times 10^{14}\,\mathrm{M}_{\odot}$) in the redshift range $z = 0.5$–0.8 to constrain the amplitude of fluctuations σ_8 within 10 per cent in the ΛCDM case. Such uncertainty in σ_8 comes from the presence of very large errors in cluster number counts, which are big enough for different models to survive. Moreover, errors in the mass determination of clusters also significantly change the expected number counts (Lima & Hu 2004).

In the near future new surveys are planned to specifically find clusters in the sky. The South Pole Telescope (SPT) (SPT Collaboration: Ruhl et al. 2004), which is currently under construction, will use the Sunayev–Zeldovich effect to find clusters and determine their masses. Also the recently proposed Dark Energy Survey (DES) (Annis et al. 2005)[2] will observe almost the same region of the sky and provide redshifts for those clusters. Both surveys will share an area of 4000 deg^2 in which 2000 clusters are expected to be found. Such large numbers will allow to better test and discriminate dark energy models. The expected errors in redshift for the SPT+DES clusters are $\sigma_z = 0.02$ for clusters with $z < 1.3$ and $\sigma_z < 0.1$ for clusters in the redshift range $1.3 < z < 2$. Where σ_z encompasses the 68 per cent probability for the redshift being in the $z \pm \sigma_z$ range.

[2]Dark Energy Survey: http://cosmology.astro.uiuc.edu/DES/ http://www.darkenergysurvey.org

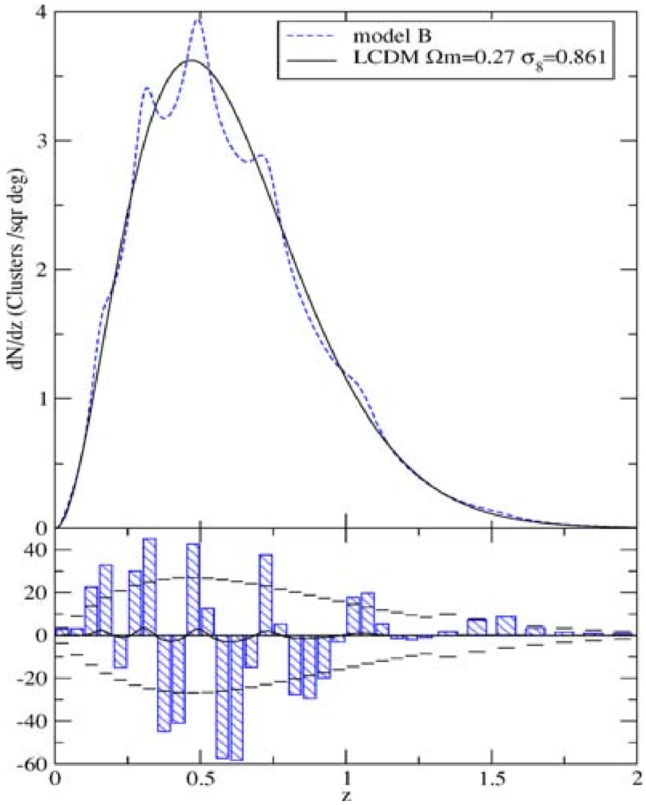

Figure 6. Top: cluster number counts for model B (dashed line) along with a ΛCDM fit for the model (solid line). The fit is done by adjusting σ_8 and Ω_m. Bottom: cluster number counts in redshift bins for the 4000 deg DES+SPT survey. Horizontal bars show shot-noise errors for the bins. Solid line shows the wiggles as a difference between model B and the fit in an arbitrary scale.

In order to explore the potential detectability of wiggles in the cluster number counts from these future surveys, we fit model B with a flat ΛCDM model by varying σ_8 and Ω_m. We simply integrate the cluster number counts for all 4000° DES+SPT survey in redshift bins. We choose to use bins of width 0.05 for $z < 1.3$ and 0.1 within the range $1.3 < z < 2$, to be consistent with the expected observational errors. The best fit is obtained by minimizing χ^2:

$$\chi^2 = \sum_{\text{bins}} \frac{\left(N_i^{\text{modelB}} - N_i^{\Lambda\text{CDM}}(\Omega_m, \sigma_8)\right)^2}{\sigma_{\text{SN}}^2}, \tag{26}$$

where N_i is the number of clusters in the ith bin and σ_i^{SN} is its shot noise error, which is the expected error in any counting statistics. The best fit corresponds to $\Omega_m = 0.27$ and $\sigma_8 = 0.861$. Both the best fit and model B are shown in the top panel of Fig. 6. In the bottom panel we plot the difference of the binned cluster counts between the model and the fit. This difference is also in redshift bins. In the bottom panel we also plot in horizontal bars the shot noise error for each bin. The continuous line represents the unbinned difference between model B and the fit. For clarity, this difference is arbitrarily scaled, it is plotted only to see the correspondence between bins, wiggles and the smoothing due to the binning.

In this section we are interested in having a broad idea about the potential detection of the cluster number counts oscillations, which are a special feature of coupled quintessence models. To answer this, one could ask how significant is the difference between the model and the fit, given the expected errors for the cluster number counts in each redshift bin. The minimum χ^2 for this realization is 47.7, which gives a probability of less than 5 per cent for the wiggles being explained by stochastic fluctuations from the best fit ΛCDM model. We also performed a Kolmogorov–Smirnov test, which is less sensitive to the tidal parts of the distribution. After smoothing the wiggles signature with a Gaussian beam of half-width = 0.05 in redshift to simulate the errors, the Kolmogorov–Smirnov test gives a probability ~6 per cent for ΛCDM being the underlying model. Hence, both the χ^2 test as well as the Kolmogorov–Smirnov test seem to indicate that future surveys could possibly detect those oscillations in the cluster abundances.

6 CONCLUSIONS

In this article we have investigated the possibility of using cluster number counts to differentiate dark energy models. In particular, we have studied quintessence models coupled to dark matter. We have also compared dark energy models that can present inhomogeneities at cluster scales, with models that are homogeneous at those small scales. The aim is to better understand the dependence of the cluster number counts on the coupling between dark energy and dark matter, and on the dark energy inhomogeneities during the non-linear regime of matter perturbations.

We have shown that there is a significant dependence of cluster number counts on dark energy inhomogeneities and on the amount of dark matter coupled to dark energy. Increasing the coupling between dark matter to dark energy reduces the cluster number counts. This effect is due to the decrease of the comoving matter density and the distinctive evolution of δ_c/σ in time. Dark energy clustering is shown to increase cluster number counts by slowing down the formation of structure. Hence, depending on the amount of coupling between dark energy and dark matter and on the clustering properties of dark energy, these effects can combine together or against each other to strongly increase or reduce cluster abundances.

Oscillations in cluster number counts in redshift are found to be a specific signature of models with dark matter coupled to dark energy. In homogeneous dark energy models, these oscillations are mainly present in background quantities, such as $\bar{\rho}_m$, while in the inhomogeneous case the oscillations also appear in perturbed quantities, like δ_c. We have shown that such fluctuations are propagated to the cluster number counts producing this very peculiar cosmological imprint.

Finally, we investigated the possibility of near future observations to discriminate among different quintessence models coupled to dark matter. As an example, we have chosen to test a particular model where dark energy is coupled to a small amount of dark matter and where dark energy is homogeneous at cluster scales. We fit this model to a flat ΛCDM model by varying σ_8 and Ω_m and minimizing χ^2. When plotting, in redshift bins, the cluster number counts for all 4000° of the DES+SPT surveys, wiggles still remain above the shot noise for some bins. In fact the null test from the χ^2 gives a probability of less than 5 per cent for these wiggles being a stochastic realization of a ΛCDM model. Hence, future surveys could possibly detect such wiggles and may be able to discriminate among dark energy models.

ACKNOWLEDGMENTS

We would like to specially thank N. J. Nunes for his data and for all his helpful comments and discussions. We also thank F. Abdalla, C. van de Bruck, F. Castander, M. Le Delliou, E. Gaztaãga, A. Lopes, R. Scoccimarro and D. Tochini-Valentini for the helpful discussions. DFM acknowledge support from the Research Council of Norway through project number 159637/V30. MM acknowledge support form Catalan Departament d'Universitats, Recerca i Societat de la Informació and from European Social Fund.

REFERENCES

Amendola L., 2000, Phys. Rev. D, 62, 043 511
Amendola L., Tocchini-Valentini D., 2001, Phys. Rev. D, 64, 043 509
Amendola L., Tocchini-Valentini D., 2002, Phys. Rev. D, 66, 043 528
Annis J. et al., 2005, White Paper submitted to Dark Energy Task Force (astro-ph/0510195)
Arbey A., Lesgourgues J., Salati P., 2001, Phys. Rev. D, 64, 123 528
Bagla J., Jassal H., Padmanabhan T., 2003, Phys. Rev. D, 67, 063 504
Bahcall A., Bode P., 2003, ApJ, 588, L1
Barreiro T., Copeland E., Edmund J., Nunes N. J., 2000, Phys. Rev, D, 61, 127 301
Barrow J. D., Mota D. F., 2003, Class. Quantum Gravity, 20, 2045
Bertolami O., Mota D. F., 1999, Phys. Lett. B, 455, 96
Bond J., Cole S., Efstathiou G., Kaiser N., 1991, ApJ, 379, 440
Brax P., Martin J., 1999, Phys. Lett. B, 468, 40
Brax P., van de Bruck C., Davis A., Khoury J., Weltman A., 2004, Phys. Rev. D, 70, 123 518
Brookfield A., van de Bruck C., Mota D. F., Tocchini-Valentini D., 2006, Phys. Rev. Lett., 96, 061 301
Carroll S. M., 1998, Phys. Rev. Lett., 81, 3067
Carroll S. M., Press W. H., Turner E. L., 1992, ARA&A, 30, 499
Causse M., 2003, A Rolling Tachyon Field for Both Dark Energy and Dark Halos of Galaxies, preprint (astro-ph/0312206)
Clifton T., Mota D. F., Barrow J. D., 2004, MNRAS, 358, 601
Copeland E. J., Nunes N. J., Pospelov M., 2004, Phys. Rev. D, 69, 023 501
Damour T., 1990, Phys. Rev. Lett., 64, 123
Damour T., Gibbons G. W., Gundlach C., 1990, Phys. Rev. Lett., 64, 123
Doran M., Karwan K., Wetterich C., 2005, J. Cosmol. Astropart. Phys., 0511, 007
Dvali G., Gabadadze G., Porrati M., 2000, Phys. Lett. B, 485, 208
Ellis J., Kalara S., Olive K., Wetterich C., 1989, Phys. Lett. B, 228, 264
Farrar G., Peebles P., 2004, ApJ, 604, 1
Ferreira P., Joyce M., 1998, Phys. Rev. D, 58, 023 503
Freese K., Lewis M., 2002, Phys. Lett. B, 540, 1
Governato F., Babul A., Quinn T., Tozzi P., Baugh C. M., Katz N., Lake G., 1999, MNRAS, 307, 949
Gross M. A. K., Somerville R. S., Primack J. R., Holtzman J., Klypin A., 1998, MNRAS, 301, 81
Haiman Z., Mohr J. J., Holder G. P., 2000, ApJ, 553, 545
Holden D. J., Wands D., 2000, Phys. Rev. D, 61, 043 506
Horellou C., Berge J., 2005, MNRAS, 360, 1393
Jassal H., Bagla J., Padmanabhan T., 2005, Phys. Rev. D, 72, 103 503
Jenkins A. et al., 2001, MNRAS, 321, 372
Kaplinghat M., Rajaraman A., 2006, preprint (astro-ph/0601517)
Khoury J., Weltman A., 2003, preprint (astro-ph/0309300
Khoury J., Weltman A., 2004a, Phys. Rev. Lett., 93, 171104
Khoury J., Weltman A., 2004b, Phys. Rev. D, 69, 044 026
Lacey C., Cole S., 1993, MNRAS, 262, 627
Le Delliou M., 2006, J. Cosmol. Astropart. Phys., 0601, 021
Lima M., Hu W., 2004, Phys. Rev. D, 70, 043 504
Lima M., Hu W., 2005, Phys. Rev. D, 72, 043006
Lopes A. M., Mota D. F., Miller L. 2004, A&A, submitted
Ma C., Caldwell R. R., Bode P., Wang L., 1999, ApJ, 521, L1
Mainini R., Bonometo S. A., 2004, Phys. Rev. Lett., 93, 121301
Maor I., Lahav O., 2005, J. Cosmol. Astropart. Phys., 0507, 003
Mota D. F., Barrow J. D., 2004a, Phys. Lett. B, 581, 141
Mota D. F., Barrow J. D., 2004b, MNRAS, 349, 281
Mota D. F., van de Bruck C., 2004, A&A, 421, 71
Multamaki T., Manera M., Gaztanaga E., 2003, MNRAS, 344, 761
Nunes N., Mota D. F., 2006, MNRAS, 368, 751
Nunes N. J., da Silva A. C., Aghanim N., 2005, preprint (astroph/0506043)
Padmanabhan T., 1995, Structure Formation in the Universe. Cambridge Univ. Press, Cambridge
Padmanabhan T., 2002, Phys. Rev. D, 66, 021 301
Padmanabhan T., Choudhury T., 2002, Phys. Rev. D, 66, 081 301
Perlmutter S. et al., 1999, ApJ, 517, 565
Press W., Schechter P., 1974, ApJ, 187, 425
Ratra B., Peebles P., 1988a, ApJ, 325, L17
Ratra B., Peebles P., 1988b, Phys. Rev. D, 37, 3406
Riess A. G. et al., 2001, ApJ, 560, 49
Riess A. G. et al. (Supernova Search Team Collaboration), 2004, ApJ, 607, 665
Ruhl J., Ade P. (SPT Collaboration), 2004, Proc. SPIE, 5498, 11
Sarkar S., 1996, Rep. Prog. Phys., 59, 1493
Schuecker P., Caldwell R. R., Böhringer H., Collins C. A., Guzzo L., Weinberg N. N., 2003, A&A, 402, 53
Sheth R. K., Tormen G., 1999, MNRAS, 308, 119
Solevi P., Mainini R., Bonometto S. A., Macciò A. V., Klypin A., Gottlöber S., 2006, MNRAS, 366, 1346
Spergel D. N. et al., 2003, ApJS, 148, 175
Springel V. et al., 2005, Nat, 435, 629
Steinhardt P., 2003, Phil. Trans. R. Soc. Lond. A, 361, 2497
Steinhardt P. J., Wang L., Zlatev I., 1999, Phys. Rev. D, 59, 123 504
Sugiyama N., 1995, ApJS, 100, 281
Tocchini-Valentini D., Amendola L., 2002, Phys. Rev. D, 65, 063 508
Viana P., Liddle A., 1999, MNRAS, 303, 535
Wang L. M., Steinhardt P. J., 1998, ApJ, 508, 483
Wang S., Khoury J., Haiman Z., May M., 2004, Phys. Rev. D, 70, 123 008
Wetterich C., 1995, A&A, 301, 321
Wetterich C., 2001, Phys. Lett. B, 522, 5
Wetterich C., 2002, Phys. Rev. D, 65, 123 512
Zehavi I. et al. (SDSS Collaboration), 2002, ApJ, 571, 172
Zlatev I., Wang L., Steinhardt P., 1999, Phys. Rev. Lett., 82, 896

This paper has been typeset from a TEX/LATEX file prepared by the author.